Supporting Information

Highly sensitive quartz crystal microbalance sensor modified with antifouling microgels for saliva glucose monitoring

Qian Dou,[a,b] Shiwen Wang,[b] Zifeng Zhang,[a,b] Yanxiang Wang,[e] Zhipeng Zhao,[b] Haijian Guo,[f] Hongliang Liu*[d] and Qing Dai*[,a,b,c]

[a.] School of Materials Science and Engineering, Zhengzhou University, Zhengzhou 450001, P. R. China.
[b.] Division of Nanophtonics, CAS key laboratory of Standardization and Measurement for Nanotechnology, CAS Center for Excellence in Nanoscience, National Center for Nanoscience and Technology, Beijing 100190, P. R. China.
[c.] Center of Materials School and Optoelectronics, University of Chinese Academy of Scienses, Beijing 100049, P. R. China.
[d.] CAS Key Laboratory of Bio-Inspired Materials and Interfacial Science, Technical Institute of Physics and Chemistry, Chinese Academy of Sciences, Beijing 100190, P. R. China.
[e.] Institute of Medicinal Biotechnology, Chinese Academy of Medical Sciences and Peking Union Medical College, Beijing 100050, China.
[f.] Jiangsu Provincial Center for Disease Control and Prevention, Nanjing 210009, P. R. China.

Sensing behaviour

QCM is a mass-sensitive sensor. It can continuously monitor the glucose concentration in a solution by recording the frequency shift (△F) of QCM chip before and after contact with the glucose-containing solution.[1,2] As shown in Figure S1a, the absolute value of △F increases when glucose molecules bind to glucose sensitive film. When testing glucose in saliva, proteins are easily adsorbed on the QCM sensor surface, resulting in inaccurate glucose detection.[3] Here, anti-fouling materials are introduced to glucose-sensitive materials, it can effectively reduce the interference of proteins on glucose detection (Figure S1b).

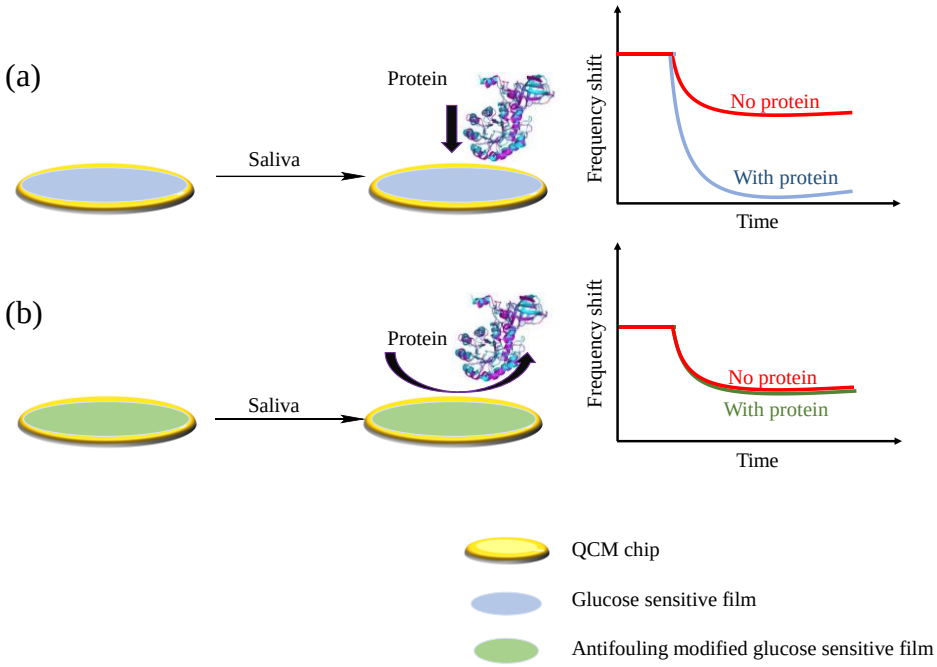

Figure S1. (a) Proteins can be adsorbed on the surface of the coated-chip when no anti-protein material is added. It will cause an increase in frequency shifts. (b) When anti-protein materials are added, the coated-chip can effectively resist the non-specific adsorption of proteins. It will not affect the frequency shifts.

The reaction principle between microgels and amino acids

The microgels@amino acids has a core-shell structure, which was synthesized by two steps. Firstly, boric acid microgels were synthesized by reflux-precipitation polymerization. Secondly, neutral amino acids were grafted onto the surface of microgels by 'click reaction'.

Neutral amino acids can exist as zwitterions with no electrical charge in aqueous solution at appropriate pH ranges. From Figure S2, when hydroxide ions are added, the pH shifts to a higher value, and the $-NH^{3+}$ groups convert to $-NH_2$ groups by removing the hydrogen ions. The nitrogens of the $-NH_2$ groups attack the epoxide groups on the surface of microgels to form secondary amino groups (−NH−) via ring-opening reaction. After that, the pH shifts to about 7 by adding hydrogen ions, and −NH− groups become protonated secondary amino cations as $-NH^{2+}-$. As the net charge of amino acids is zero in the appropriate pH range of about 7, the amino acids layer on the surface of microgels are obtained.[4]

The reaction solvent for grafting amino acids onto the surface of microgels was ethanol solution ($V_{ethanol}$: V_{water} = 1: 3), and the microgels were in a swollen state. Amino acids are small molecules that can easily penetrate into the microgels. In addition, the activity of the 'click reaction' between amino groups and epoxy groups is high. Therefore, amino acids exist not only on the surface of the microgels but also inside of the microgels.[4]

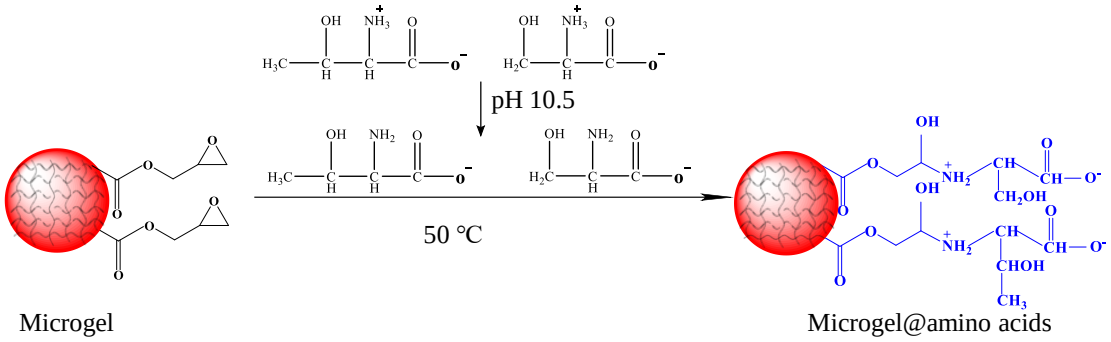

Figure S2. The 'click reaction' between microgels and amino acids.

AFM of microgels

In order to observe the microgels after incubation with aqueous solution by atomic force microscopy atomic force microscopy (AFM), aqueous solution was dropped onto the surface of the microgels-coated chip. When the microgel is in dry state, the surface of microgel is uneven (Figure S3a). While, the microgel displays many regular holes ~5 nm in diameter (Figure S3b) upon exposure of aqueous solution. In addition, the height of microgel in aqueous solution is 3.5 times than its in dry condition.

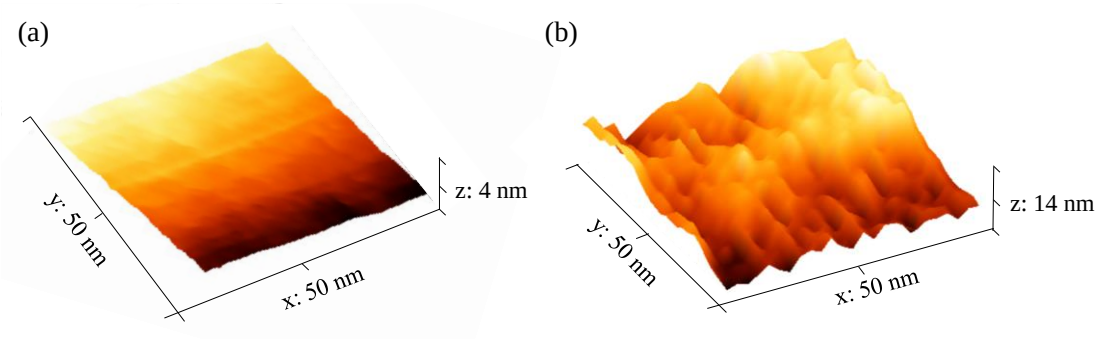

Figure S3. (a) AFM of the microgels in dry state. (b) AFM image of the microgels after incubation with aqueous solution.

Cross-linking mechanism of microgels @ amino acids

The pre-polymer solution was composed of microgels@amino acids, N-vinylpyrrolidone (NVP), ethyleneglycol dimethacrylate (EGDMA) and 2,2-dimethoxy-1,2-diphenyl-ethanone (DMPA). NVP, EGDMA and DMPA were used as monomer, crosslinking agent and initiator, respectively. After absorbing ultraviolet light, the initiators transit from the ground state to the excited state, and then undergo molecular cleavage to form free radicals, which ultimately initiate the polymerization reaction.[5] Microgels@amino acids particles can be directly cross-linked together via chemical (covalent bond formation) forces to form a microgel network on the double-

bonded QCM chip. By reducing the film thickness, the SEM of microgels@amino acids@cross-linked-coated chip is consistent with the description of the literature (Figure S4).[6]

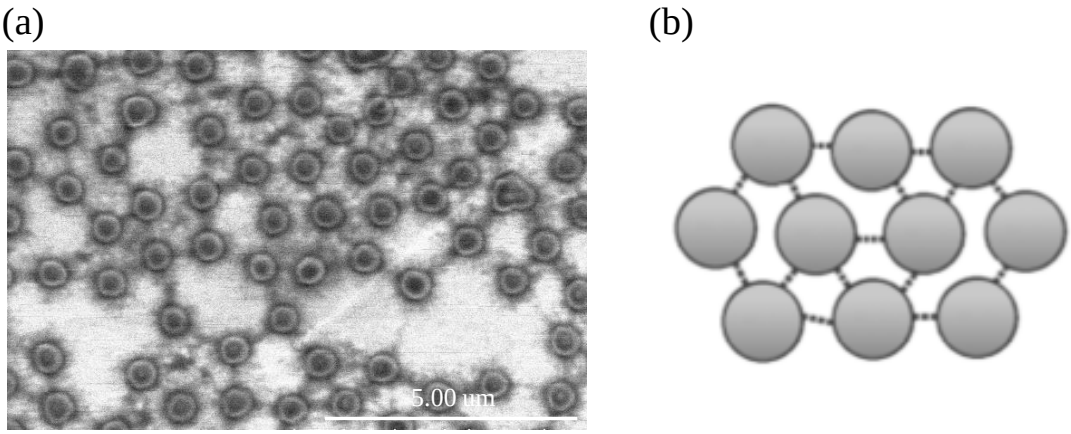

Figure S4. (a) The SEM of microgels@amino acids@cross-linked-coated chip. (b) Schematic diagram of direct microgels crosslinking from reference 6.

Comparison of antifouling performance

In order to prove the antifouling performance of the microgels@amino acids@crosslinked layer-coated sensors, the microgels-coated sensors and microgels@crosslinked layer-coated sensor are used as comparative experiments. From Figure 4a, b, Figure S5a, b, c, d and Table S1, the microgels@amino acids@crosslinked layer-coated sensors had the best resistance to BSA, LYS, FIB and MUC. For BSA, LYS and MUC, the anti-protein performance of the microgels@crosslinked layer-coated sensor was superior to that of the microgels-coated sensor. Therefore, the superior anti-protein performance of microgels@amino acids@crosslinked layer-coated sensor mainly benefits from the amino acids layer and crosslinking layer.

For organic molecular interference, L-DOPA and AA had greater influence on microgels-coated sensors. It may be because their structures contain cis hydroxyl groups, which are easy to combine with boric acid groups. While, when microgels were modified by the cross-linking layer, the influence of L-DOPA and AA on sensors reduced drastically. L-DOPA contains amino and carboxyl groups, which is similar to the structure of protein. Therefore, the mechanism of resistance is similar to that of proteins. For AA, it has a cyclolactone. The cross-linked layer has polyvinyl pyrrolidone, which contains many polar lactam groups, not easy to combine with AA. These three types of sensors have superior resistance to UREA, GSH, UA and CRE, and the absolute value of the average of frequency displacement were all less than 20 Hz.

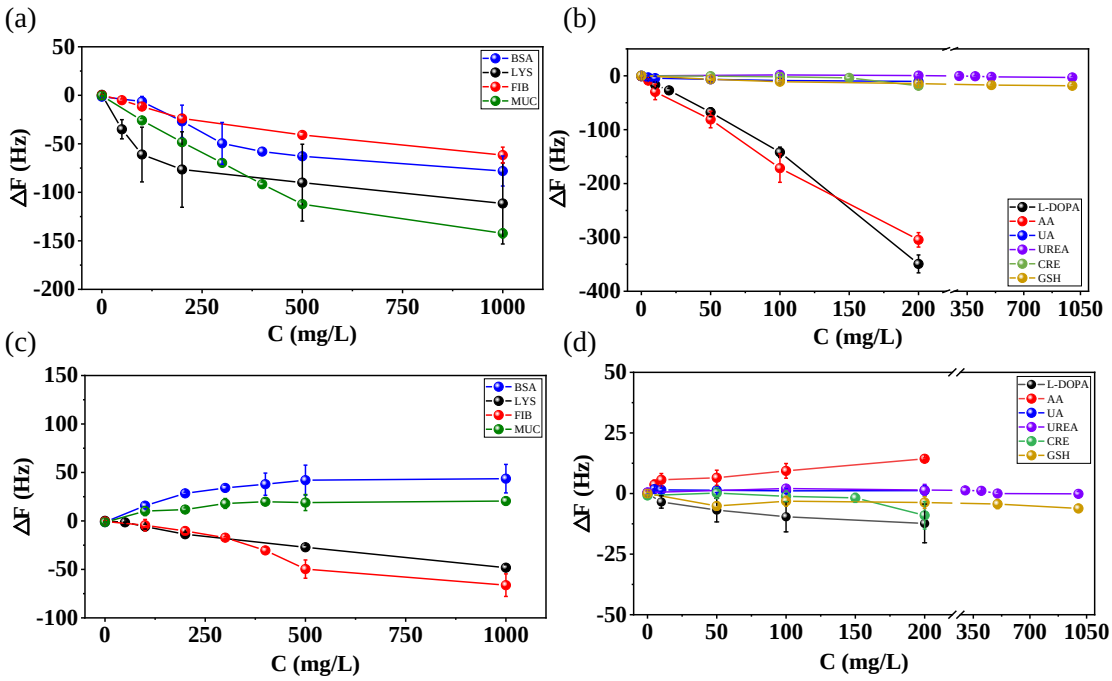

Figure S5. (a) Effects of proteins (BSA, MUC, FIB and LYS) on microgels-coated sensors. (b) Effects of organic molecules (GSH, UREA, CRE, UA, AA and L-DOPA) on microgels-coated sensors. (c) Effects of proteins (BSA, MUC, FIB and LYS) on microgels@crosslinked layer-coated sensors. (d) Effects of organic molecules (GSH, UREA, CRE, UA, AA and L-DOPA) on microgels@crosslinked layer-coated sensors.

Table S1. The anti-pollution comparison of microgels-coated sensors, microgels@crosslinked layer-coated sensors and microgels@amino acids@crosslinked layer-coated sensors.

Interfering substance	Concentration (mg/L)	Film	The absolute value of the average of △F (Hz)
BSA	1000	microgels	78.0
		microgels@crosslinked layer	43.6
		microgels@amino acids@crosslinked layer	10.6
LYS	1000	microgels	111.5
		microgels@crosslinked layer	48.2
		microgels@amino acids@crosslinked layer	38.5
FIB	1000	microgels	61.6
		microgels@crosslinked layer	66.2
		microgels@amino acids@crosslinked layer	5.7
MUC	1000	microgels	142.2
		microgels@crosslinked layer	20.5
		microgels@amino acids@crosslinked layer	9.3
		microgels	3.1

UREA	1000	microgels@crosslinked layer	0.2
		microgels@amino acids@crosslinked layer	6.9
GSH	1000	microgels	18.4
		microgels@crosslinked layer	6.1
		microgels@amino acids@crosslinked layer	0.5
L-DOPA	200	microgels	349.2
		microgels@crosslinked layer	12.3
		microgels@amino acids@crosslinked layer	13.8
AA	200	microgels	304.5
		microgels@crosslinked layer	14.3
		microgels@amino acids@crosslinked layer	14.0
UA	200	microgels	10.3
		microgels@crosslinked layer	1.2
		microgels@amino acids@crosslinked layer	5.2
CRE	200	microgels	18.5
		microgels@crosslinked layer	9.0
		microgels@amino acids@crosslinked layer	1.1

Literature contrast

Table S2 summarizes the characteristics of glucose sensors. At present, antifouling sensors are mainly based on blood glucose sensors. Particularly, for the QCM glucose sensor, our sensor and reference 22 can meet the detection of saliva glucose range (0–40 mg/L). Regarding the detection specimen, reference 21 and 22 involved the detection of serum glucose.

In reference 21, a 600–800 nm (3-acrylamidopropyl) tri-methylammonium chloride modified poly(acrylamide-co-3-acrylamideophenylboronic acid) hydrogel film was coated on the quartz disc for glucose sensing. The linear relationship between the dissipation response and the glucose concentration was achieved in the range of 0 to10 mM (0–1801.6 mg/L). The responses to glucose of the sensor has been measured under human serum with glucose concentrations in 2.48 mM (446.8 mg/L), 5.06 mM (911.6 mg/L) and 9.93 mM (1796.2 mg/L). This work detected the glucose concentration in the blood glucose range, the material has not been treated with antifouling material and only the performance of high concentration glucose in the serum was tested. In reference 22, a series of cyclic peptide (CP) glucose receptors were designed to mimic the binding sites of glucose binding protein (GBP), the properties of these CPs used as a glucose receptor or substitute for the GBP were studied by using QCM. The glucose detection range was 10 nM–20 mM (0.18–3603.2 mg/L) in PBS and different glucose concentrations (0.01 mmol/L (1.8 mg/L), 0.1 mmol/L (18.0 mg/L), 0.5 mmol/L (90.1 mg/L), 1 mmol/L (180.2 mg/L), 2 mmol/L (360.3 mg/L)) were measured at diluted human serum samples (1:10 in PBS). Although this work could detect the glucose concentration in the saliva glucose range, the material has not been treated with antifouling material and the detection of glucose in serum samples (1:10 in PBS) was tested. The article also proposed that proteins in human

serum bind nonspecifically and interfere with or inhibit CP-3/glucose interactions to produce false positive assay results.

In this work, we designed a QCM glucose sensor with protein-resistive function to achieve the high-sensitivity detection of saliva glucose. Microgel containing boric acid segments was used as multi-binding sites for glucose and amino acid layer and crosslinking layer were used as the protein-resistive component. The designed QCM sensor has a good linearity in the glucose concentration range of 0–40 mg/L and the glucose sensor could detect the 50% saliva glucose (glucose concentration 100 mg/L, 200 mg/L, 500 mg/L).

Table S2. Summary of literatures on glucose sensors.

Detection method	pH	Detection range	Detection limit	Specimen	Reference
Electrochemistry	7.4	0.2–5 mM (36.0–900.8 mg/L)	0.05 mM	PBS, 100% bovine serum	7
Electrochemistry	—	4–20 mM (720.6–3603.2 mg/L)	—	PBS, 100% human blood serum	8
Electrochemistry	7.4	2−30 mM (360.3−5404.8 mg/L)	—	PBS, Porcine serum	9
Electrochemistry	7.4	50−400 mg/dL (500−4000 mg/L)	—	PBS, Human serum.	10
Electrochemistry	7.0	0−14 mM (0−2522.2 mg/L)	—	PBS， Bovine serum	11
Electrochemistry	7.4	4−20 mM (720.6−3603.2 mg/L)	—	PBS, 10%, 50%， 100% human blood serum	12
eQCM	—	1−20 mM (180.2−3603.2 mg/L)	—	PBS, 100% human blood serum	13
QCM	9.0	5–100 mmol/L (900.8–18016.0 mg/L)	—	PBS	14
QCM	10.0	0.07–8 mmol/L (12.6–1441.3 mg/L)	0.07 mmol/L (12.6 mg/L)	PBS	15
QCM	7.0–7.5	1.1–33.3 mmol/L (198.2–5999.3 mg/L)	20 μmol/L (3.6 mg/L)	PBS	16

QCM	9.5	0.05 g/dL–0.14 g/dL (500–1400 mg/L)	—	PBS	17
QCM	9.0	0–10 mmol/L (0–1801.6 mg/L)	—	PBS	18
QCM	7.4	0–30 mmol/L (0–5400.5 mg/L)	—	PBS	19
QCM	7.0	0.08–10 mmo/L (14.4–1801.6 mg/L)	80 µmol/L (14.4 mg/L)	PBS	20
QCM	7.4	0–10 mmol/L (0–1801.6 mg/L)	1 mmol/L (180.16 mg/L)	PBS and human serum	21
QCM	7.4	10 nmol/L–20 mmol/L (0.18–3603.2 mg/L)	—	PBS and diluted human serum samples (1:10 in PBS)	22
QCM	6.8–7.5	0–40 mg/L	5 mg/L	PBS and diluted human saliva samples (1:1 in PBS)	Our work

Notes and references

1. J. Mandal, A. Arcifa and N. D. Spencer, *Polym. Chem*., 2020, **11**, 3209–3216.
2. Ö. Ertekin, S. Öztürk and Z. Z. Öztürk, *Sensor*, 2016, **16**, 1274.
3. Y. C. Hu, B. Liang, L. Fang, G. G. Ma, G. Yang, Q. Zhu, S. F. Chen and X. S. Ye, *Langmuir*, 2016, **32**, 11763–11770.
4. C. Xu, X. Hu, J. Wang, Y. M. Zhang, X. J. Liu, B. B. Xie, C. Yao, Y. Li and X. S. Li, *ACS Appl. Mater. Interfaces*., 2015, **7**, 17337−17345.
5. J. Y. Ma, K. Fu, Y. L. Zhang, C. Qin and X. N Zhao, *Chemical Research and Application*, 2015, **27**, 1574–1580.
6. T. Farjami and Ashkan Madadlou, *Food Hydrocolloids*, 2017, **62**, 262–272.
7. Y. C. Hu, B. Liang, L. Fang, G. L. Ma, G. Yang, Q. Zhu, S. F. Chen and X. S. Ye, *Langmuir*, 2016, **32**, 11763–11770.
8. W. Yang, T. Bai, L. R. Carr, A. J. Keefe, J. J. Xu, H. Xue, C. A. Irvin, S. F. Chen, J. Wang and S. Y. Jiang, *Biomaterials*, 2012, **33**, 7945−7951.

9. S. Vaddiraju, Y. Wang, L. Qiang, D. J. Burgess and F. Papadimitrakopoulos, *Anal. Chem.*, 2012, **84**, 8837−8845.
10. J. H. Han, J. D. Taylor, D. S. Kim, Y. S. Kim, Y. T. Kim, G. S. Cha and H. Nam, *Sensors and Actuators B*, 2007, **123**, 384–390.
11. L. Fang, B. Liang, G. Yang, Y. C. Hu, Q. Zhu and X. S. Ye, *Biosens. Bioelectron.*, 2014, **56**, 91–96.
12. W. Yang, H. Xue, L. R. Carr, J. Wang and S. Y. Jiang, *Biosens. Bioelectron*., 2011, **26**, 2454–2459.
13. H. Y. Wu, C. J. Lee, H. F. Wang, Y. Hu, M. G. Young, Y. Han, F. J. Xu, H. B. Cong and G. Cheng, *Chem. Sci*., 2018, **9**, 2540–2546.
14. C. Sugnaux and H. A. Klok, Macromol. *Rapid. Comm.*, 2014, **35**, 1402–1407.
15. A. Ersöz, A. Denizli, A. Özcan and R. Say, *Biosens. Bioelectron*., 2005, **20**, 2197–2202.
16. Q. Dou, D. D. Hu, H. K. Gao, Y. M. Zhang, A. K. Yetisen, H. Butt, J. Wang, G. J. Nie and Q. Dai, *RSC Adv*., 2017, **7**, 41384–41390.
17. C. Y. Cho, Master of Science, Department of Chemistry University of Alberta, 2015.
18. N. Fortin and H. A. Klok, *ACS Appl. Mater. Interfaces*, 2015, **7**, 8, 4631–4640.
19. Y. Liu, D. S. Yu, C. Zeng, Z. C. Miao and L. M. Dai, *Langmuir*, 2010, **26**, 6158–6160.
20. T. Juřík and P. Skládal, *Chemical Papers*, 2015, **69**, 167–175.
21. D. Q. Chen, H. Y. Li, X. F. Su, N. Li, Y. Wang, A. C. Stevenson, R. F. Hu and G. Li, *Sensors and Actuators: B. Chemical*, 2019, **287**, 35–41.
22. C. Li, X. Chen, F. Y. Zhang, X. X. He, G. Z. Fang, J. F. Liu and S. Wang, *Anal. Chem*. 2017, **89**, 10431−10438.